AGU ADVANCING EARTH AND SPACE SCIENCES

Geophysical Research Letters®

RESEARCH LETTER
10.1029/2024GL113257

The Role of Vapor Pressure Deficit in the CLM Simulated Interaction Between Urban Heat Islands and Heat Waves Over CONUS

Linying Wang[1,2], Dan Li[2], and Xing Yuan[1]

[1]National Key Laboratory of Earth System Numerical Modeling and Application, Institute of Atmospheric Physics, Chinese Academy of Sciences, Beijing, China, [2]Department of Earth and Environment, Boston University, Boston, MA, USA

Key Points:

- The daily urban heat island (UHI) intensity increases under heat waves (HWs) over the eastern and western U.S. but decreases in the Central U.S.
- Changes in the urban and rural turbulent heat fluxes are consistent with changes in the daily mean UHI intensity
- Sensitivity of urban and rural evapotranspiration to various environmental stresses, including vapor pressure deficit, is the key to understanding UHI and HWs interactions

Supporting Information:

Supporting Information may be found in the online version of this article.

Correspondence to:

D. Li,
lidan@bu.edu

Citation:

Wang, L., Li, D., & Yuan, X. (2025). The role of vapor pressure deficit in the CLM simulated interaction between urban heat islands and heat waves over CONUS. *Geophysical Research Letters*, *52*, e2024GL113257. https://doi.org/10.1029/2024GL113257

Received 28 OCT 2024
Accepted 22 FEB 2025

Abstract Although both urban and rural temperatures are expected to increase under heat waves (HWs), whether the urban heat island (UHI) intensity becomes stronger under HWs remains unknown especially at the daily mean and large spatial scales. Using an urbanized land surface model, we quantify the interactions between UHIs and HWs over the Contiguous United States (CONUS). Synergistic interactions (i.e., increased UHI intensities under HWs) are observed over the eastern and western U.S. However, negative interactions are found in the Central U.S. due to the stronger inhibition of rural evapotranspiration by vapor pressure deficit (VPD) stresses. The interactions between UHIs and HWs in the Central U.S. will be further reduced along with the elevated VPD stresses in a hotter future. The results highlight the importance of properly parameterizing the sensitivity of urban and rural evapotranspiration to various environmental stresses in climate and earth system models.

Plain Language Summary The combination of heat waves (HWs) and urban heat island (UHI) effects represents the worst scenario for urban residents in terms of heat-related health risks. This is especially true when the UHI intensity is further exacerbated by HWs, namely, when urban temperature increases under HWs are stronger than their rural counterparts. Using a state-of-the-art land surface model, we investigate whether the UHI intensity is enhanced under HWs and find non-uniform results over the Contiguous United States. Our study has implications for understanding the spatiotemporal variability of UHI-HW interactions and for improving climate and earth system models.

1. Introduction

More than 50% of the global population live in cities, making urban areas a critical nexus of water, energy, and health challenges facing humanity (Grimm et al., 2008). A better understanding of the urban microclimate is the key to tackling these challenges (Grimmond, 2007). Most cities experience the so-called urban heat island (UHI) effect with higher temperatures than the surrounding areas (Oke, 1982). The UHI effect is arguably one of the most significant human-induced changes to Earth's surface climate (Kalnay & Cai, 2003; Li et al., 2019; Manoli et al., 2019; L. Zhou et al., 2004; Zhao et al., 2014).

There are many causes of the UHI effect, including limited green spaces, modified surface hydrothermal properties with man-made materials, complex canopy geometries, as well as large anthropogenic heat fluxes in cities (Oke et al., 2017). The UHI intensity often exhibits strong spatial (Li et al., 2019; Manoli et al., 2019; Zhao et al., 2014) and temporal (D. Zhou et al., 2016; Manoli et al., 2020) variability. In terms of temporal variations, numerous studies have examined the diurnal and seasonal variations of UHI intensity. However, the day-to-day variations of UHI intensity are relatively less studied (Li et al., 2024), even though empirical evidence showed that the UHI intensity is modulated by weather variables such as cloud cover and wind speed that exhibit strong day-to-day variations (Arnfield, 2003; Oke et al., 2017).

Of particular interest is how the UHI intensity is affected by heat waves (HWs), which are excessively hot periods lasting for several days or longer and are typically caused by slow-moving high pressure systems (Perkins, 2015). Heat waves are amongst the deadliest natural disasters since heat is the most important cause of weather-related mortality (Hajat & Kosatky, 2010). If the UHI intensities were enhanced under HWs compared to non-HW (typical summer) conditions, namely, the increases of urban temperatures due to HWs are stronger than those of rural temperatures, urban residents would face even higher heat-related health risks. Studies have found a

2.49% increase in mortality risk for every 1°F increase in HW intensity in the United States (Anderson & Bell, 2011). This synergistic combination of HWs and UHIs also poses serious challenges for air quality management, electric systems, and water infrastructure.

However, whether the UHI intensity under HWs is higher or lower than that under non-HW conditions remains under debate (see a recent review by Kong et al., 2021). Many studies reported that UHI intensities are enhanced under HWs conditions (e.g., Ao et al., 2019; Founda & Santamouris, 2017; Li & Bou-Zeid, 2013; Li et al., 2015; Ramamurthy & Bou-Zeid, 2017; Schatz & Kucharik, 2015), but some studies reported no or negative interactions (e.g., Chew et al., 2021; Kumar & Mishra, 2019; Richard et al., 2021; Scott et al., 2018). Moreover, there exist important research gaps. First, most previous studies focus on a single city/metropolitan region and one single to a few HW events. Large-scale investigations that compare UHI and HW interactions across different places and multiple HWs are relatively sparse, with the exception of the study by Zhao et al. (2018) which investigated interactions between UHIs and HWs over 50 cities in the U.S. Second, many studies separate daytime and nighttime UHIs and examine their interactions with HWs separately (e.g., Zhao et al., 2018), but investigations of the daily mean UHI are rare. Notwithstanding the importance of understanding the diurnal behavior of UHIs, we argue that it is also important to examine the daily mean UHI since HWs are weather phenomena present in both daytime and nighttime.

In this study, we aim to bridge these research gaps by investigating UHI and HW interactions at the continental (over the Contiguous United States or CONUS) and daily mean scales. We focus on addressing the following questions: (a) does the daily mean UHI intensity increase or decrease under HWs? (b) what are the mechanisms that cause positive and negative interactions at the daily mean scale?

2. Methodology

We use the Community Land Model (CLM), which is the land component of the Community Earth System Model (CESM) (Danabasoglu et al., 2020). In this study, the CLM version 5 (CLM5) in CESM2.1.3 is used. In each grid cell, CLM employs a subgrid approach to distinguish different land cover types, including natural vegetation, crop, urban, lake, and glacier. The natural vegetation and crops are treated as rural land. Urban climate processes are parameterized by the Community Land Model-Urban (CLMU), which follows the urban canyon concept. In this framework, heat fluxes from different urban surfaces interact within a bulk urban air mass that represents the air in the urban canopy layer for which the near-surface air temperature is computed. Additionally, a new building energy model has been developed for CLM5, which computes interior building air temperature and provides more realistic energy use for heating and air conditioning. CLMU also allows for the simulation of multiple urban density classes (i.e., tall building district, high density, and medium density) within each grid cell. A more detailed description can be found elsewhere (Oleson, Bonan, Feddema, & Vertenstein, 2008; Oleson, Bonan, Feddema, Vertenstein, et al., 2008; Oleson, Bonan, Feddema, Vertenstein, & Kluzek, 2010; Oleson & Feddema, 2020). The CLMU model has been widely used to study UHIs (Oleson et al., 2011; Zhao et al., 2014), as well as urban heat mitigation (Oleson, Bonan, & Feddema, 2010; L. Wang et al., 2020, 2021).

We run CLM5 in an offline mode (i.e., forced by hourly meteorological data) at a spatial resolution of 1/8 degree over CONUS. Three 40 year numerical experiments are conducted, including two historical experiments (1980–2019) and one future experiment (2060–2099) under the Representative Concentration Pathway (RCP) 8.5. The two historical experiments differ in terms of whether irrigation for crops is turned on or not. For the future experiment, the irrigation is turned on. The historical and future meteorological forcings are derived from the high-resolution (12 km) hourly IM3/HyperFACETS product (Jones et al., 2023). The historical forcings are the dynamically downscaling results using the Weather Research and Forecasting (WRF) model, driven by the ERA5 reanalysis data. Future forcings (RCP8.5 hotter) are generated by perturbed thermodynamics experiments, again using the ERA5 historical data but with the added climate change signals. More details on the forcing data are available on the IM3/HyperFACETS data website (https://tgw-data.msdlive.org/). Before we perform each experiment, the model is spun up for 80 years by recycling the forcing twice. Our analysis only focuses on summer (June, July, August) days. While the meteorological conditions from WRF simulations consider some urban influences, they provide the same atmospheric forcing at a reference height shared by both urban and rural patches within a CLM grid cell. CLM then simulates urban and rural temperatures separately and calculates their difference to represent the UHI intensity within the same grid cell. Therefore, the UHI intensity considered in this

10.1029/2024GL113257

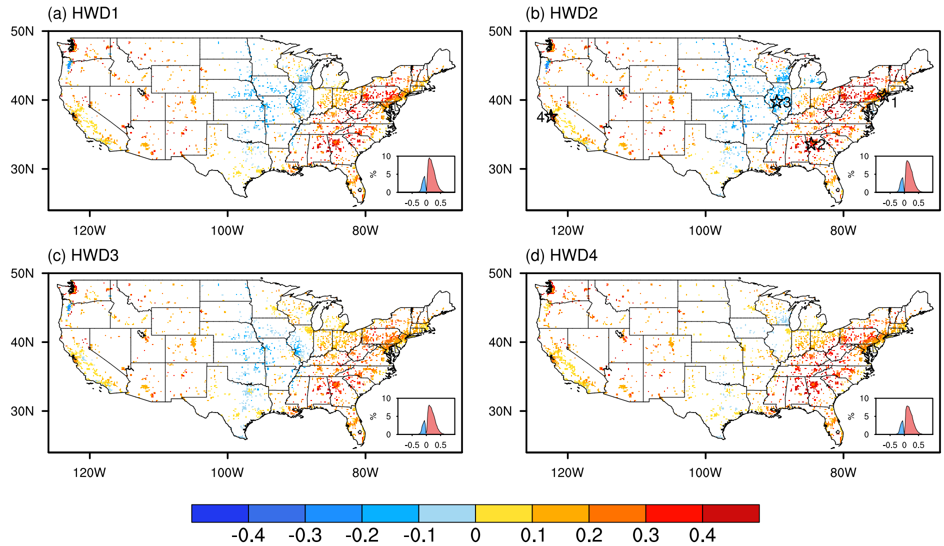

Figure 1. Changes in the daily mean urban heat island (UHI) intensity between heat wave (HW) and non-HW conditions (δUHII, unit: K). (a–d) Use four different HW definitions (HWD). Only grid cells with significant changes at the 95% confidence level in the UHI intensity and with more than 0.1% urban land are shown. The insets present the histogram (normalized by the total number of valid data, *y*-axis unit: %) of the changes in the daily mean UHI intensity between HW and non-HW conditions (*x*-axis unit: K). In (b), four points are selected to highlight the variability of changes in urban/rural latent heat flux in response to HWs in Figure S3 in Supporting Information S1.

study (i.e., difference between urban and rural patches within a CLM grid cell) is different from the urban signals in the meteorological forcing.

Heat waves are identified using different definitions. Four representative ones (Meehl & Tebaldi, 2004; Anderson & Bell, 2011; Lau & Nath, 2014; Y. Y. Chen & Zhai, 2017) are used in this work (Table S1 in Supporting Information S1), although the key findings are similar across the tested definitions. The daily maximum temperature of the meteorological forcing is used to define HWs. We also use the daily maximum temperature of the rural land and the results are extremely similar, which is expected since most grid cells have over 95% of the land area covered by rural vegetation. A Student's *t*-test is conducted to assess the statistical significance of the difference in daily mean UHI intensity between HW and non-HW days throughout the entire study period.

Unlike the work by Zhao et al. (2018) where 50 large cities over the U.S. are studied, here we investigate all grid cells where the urban land fraction exceeds 0.1% of the total land area of the grid cell. This allows us to retain small cities/towns in our analysis and yields in total 5,410 grid cells.

3. Results

Figure 1 shows changes in the daily mean UHI intensity (UHII) between HW and non-HW conditions (δUHII, where δ refers to HW minus non-HW) using four HW definitions (HWD), with values ranging primarily between −0.25 and 0.5 K. Here only grid cells with significant changes at the 95% confidence level in the UHI intensity are shown. It is clear that the changes are largely positive over CONUS (especially in the eastern U.S.), suggesting synergistic interactions between UHIs and HWs. However, negative (or no as in HWD4) interactions are observed in the Central U.S. This pattern (i.e., positive values in eastern and western U.S. but negative or close to zero values in the Central U.S.) is broadly consistent across the four HW definitions.

This pattern is consistent with changes in the surface energy budget $SW_{net} + LW_{net} + AH = H + LE + G$ as shown in Figure 2. Here SW_{net} is the net (or absorbed, incoming minus outgoing) shortwave radiation, LW_{net} is the net (i.e., incoming minus outgoing) longwave radiation, AH is the anthropogenic heat flux which is calculated as the sum of the heat removed by air conditioning and the waste heat from building heating/air-conditioning based on a sophisticated building energy model (Oleson & Feddema, 2020), H is the sensible heat flux, LE is the latent heat flux, and G is the ground heat flux into or from urban surfaces. In particular, the partition of available energy into sensible and latent heat fluxes largely explains the spatial pattern of δUHII. The spatial correlation between

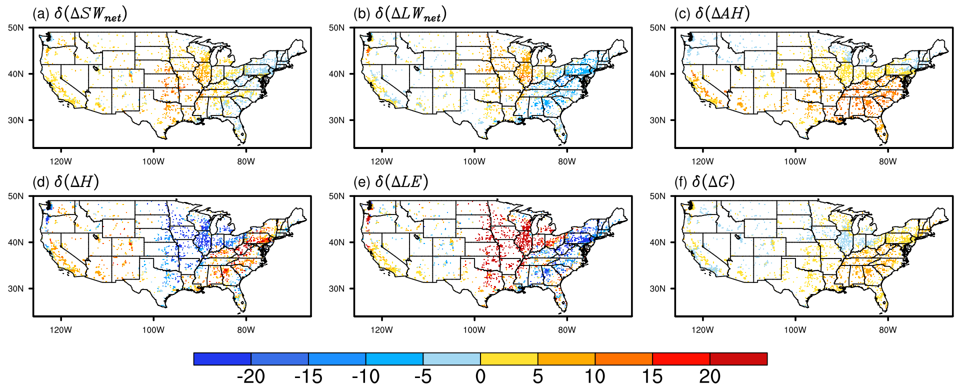

Figure 2. Changes (δ) in the urban-rural difference (Δ) of the surface energy budget between heat wave and non-HW conditions (unit: Wm^{-2}). (a–f) Present changes in the net shortwave radiation, net longwave radiation, anthropogenic heat flux, sensible heat flux, latent heat flux, and ground heat flux, respectively. Here HWD2 is used. Only grid cells with significant changes at the 95% confidence level in the urban heat island intensity and with more than 0.1% urban land are shown.

δUHII and $\delta(\Delta LE)$ ($\delta(\Delta H)$) is -0.88 (0.78), where Δ refers to the urban-rural difference (urban minus rural). Note that urban land also evaporates due to evaporation from impervious surfaces (e.g., ponding after rainfall) and soil evaporation from the pervious ground within the urban canyon.

In the eastern U.S., $\delta(\Delta LE)$ are of negative values (Figure 2e), suggesting that ΔLE decreases under HWs. Here ΔLE is a negative value because urban land evaporates less than rural land, so a smaller ΔLE corresponds to a more negative value, indicating even less evaporation over urban land. Close inspection reveals that the negative $\delta(\Delta LE)$ is because the rural latent heat flux increases more than the urban latent heat flux under HWs, leading to smaller ΔLE under HWs. Note that both urban and rural land tend to experience higher potential evaporation under HW conditions. However, whether urban or rural land increases its actual evapotranspiration also depends on how HWs affect the environmental stresses such as soil moisture and vapor pressure deficit (VPD). In the northeastern U.S. where there is generally ample rainfall during the summer, the rural land enhances its actual evapotranspiration under HWs more than the urban land (cf. Figures S1d and S1c in Supporting Information S1, see also results for point 1 in Figure S4 in Supporting Information S1). In the southeastern U.S., the rural land reduces its actual evapotranspiration under HWs less than the urban land (cf. Figures S1d to S1c in Supporting Information S1, see also results for point 2 in Figure S4 in Supporting Information S1). Hence, relative to urban evaporation, the rural evapotranspiration is enhanced (i.e., decreased ΔLE) under HWs for both northeastern and southeastern U.S. As a consequence, the urban land increases its sensible heat flux more than the rural land (Figure S1 in Supporting Information S1), resulting in large positive values of $\delta(\Delta H)$ as shown in Figure 2d.

In the western U.S. especially in California, $\delta(\Delta LE)$ are close to zero or slightly positive (see also results for point 4 in Figure S4 in Supporting Information S1). Interestingly, $\delta(\Delta H)$ are also of positive values (i.e., increased ΔH under HWs). The positive $\delta(\Delta H)$ suggests that relative to rural land, urban land enhances its sensible heat flux under HWs. The fact that both $\delta(\Delta LE)$ and $\delta(\Delta H)$ are slightly positive is due to the increased available energy in urban areas from more absorbed shortwave radiation (Figure 2a) resulting from less cloud and lower albedo, along with the additional heat from anthropogenic heat flux (Figure 2c).

In the Central U.S., large positive values of $\delta(\Delta LE)$ are observed, suggesting that ΔLE are increased under HWs. Concomitantly, ΔH are reduced under HWs. When the urban and rural latent heat fluxes are examined separately, we find that the urban and rural latent heat fluxes are both inhibited under HWs in this region, with the rural latent heat flux inhibited more than the urban latent heat flux (Figure S1 in Supporting Information S1, see also results for point 3 in Figure S4 in Supporting Information S1). Why is this case?

First, we hypothesize that this behavior is unique to crops since in this region the rural vegetation is dominated by crops. However, when the natural vegetation and crops are separately examined, it is found that both natural vegetation and crops show stronger inhibition of evapotranspiration in this region (cf. Figures S2d to S2e in Supporting Information S1) when compared to urban evaporation.

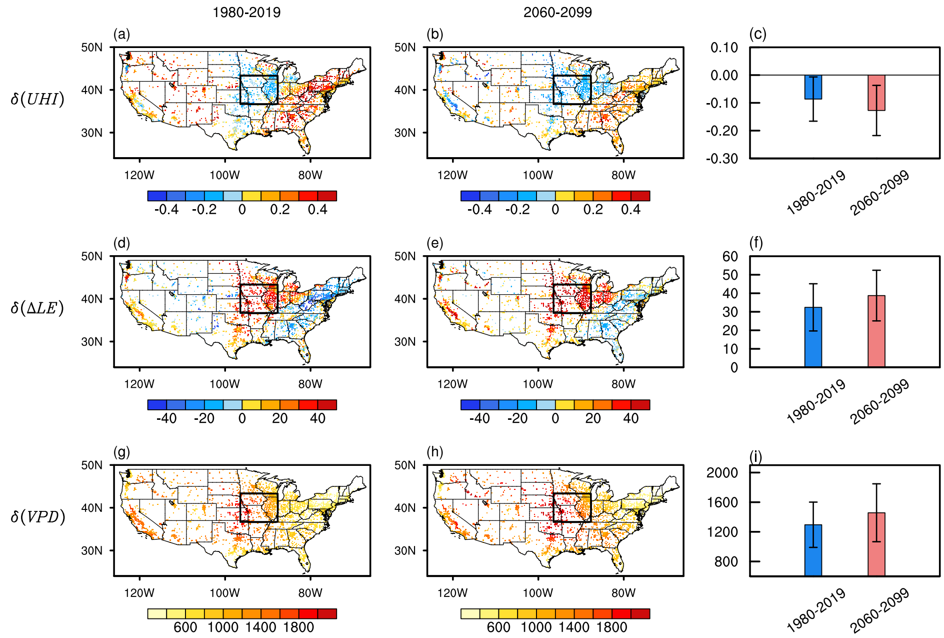

Figure 3. Changes in the urban heat island intensity (a to c, unit: K), changes in the urban-rural difference of latent heat flux (d to f, unit: Wm^{-2}), and changes in the vapor pressure deficit (g to i, unit: Pa) (c, f, i) are results for the Central U.S. represented by the black box in (a,b,d,e,g,h).

Second, we hypothesize that this behavior is due to the much stronger soil moisture stress for rural evapotranspiration under HWs than for urban evaporation. To test this hypothesis, we examine the soil water content (SWC) of the urban pervious ground and the SWC of the rural land at 10 cm (Figure S3 in Supporting Information S1). We find that both the urban and rural SWC values decrease under HWs (Figures S3a and S3b in Supporting Information S1). However, the decrease of rural soil moisture is actually weaker than that of the urban soil moisture in some parts of the Central U.S., resulting in negative values of $\delta(\Delta SWC)$. This result thus does not support the hypothesis that rural evapotranspiration experiences stronger soil moisture stress. To further corroborate this, we perform a sensitivity experiment where irrigation is turned on for the crops. When compared to results where the crops are not irrigated (cf. Figures S2e to S2f in Supporting Information S1), we find that the key finding remains unchanged in the Central U.S. This also suggests that the negative interactions between UHIs and HWs in this region are not because of stronger soil moisture stresses for rural vegetation.

Lastly, we hypothesize that non-soil moisture stresses (in particular, stresses from VPD) are the key to understanding the negative interactions between UHIs and HWs in the Central U.S. This hypothesis is motivated by that rural evapotranspiration experiences stresses from VPD through the parameterization of stomatal conductance, while such effects are absent in the urban evaporation parameterization. In rural areas, evapotranspiration is partitioned into soil evaporation, canopy evaporation, and transpiration, with stomatal conductance for transpiration calculated based on the Medlyn conductance model, which performs well at low humidity levels (Medlyn et al., 2011; Rogers et al., 2017). In urban areas, however, the effect of vegetation is parameterized using a simplified bulk scheme, where evaporation depends on the wetness of the entire soil column (Oleson, Bonan, Feddema, Vertenstein, et al., 2008). This hypothesis is also motivated by previous studies that highlight the key role of VPD in modulating the evapotranspiration response to HWs (e.g., Miralles et al., 2019; P. Wang et al., 2019; Vahmani et al., 2022). To test this, we find that δVPD is relatively higher in the Central U.S. than in other regions (Figure 3g, see also results for point 3 in Figure S4 in Supporting Information S1), consistent with the stronger increase of $\delta(\Delta LE)$ (Figure 3d). The spatial correlation between δVPD and $\delta(\Delta LE)$ is 0.5, much higher than any other environmental variables.

This raises the question of how interactions between UHIs and HWs in this region will evolve in future climates, as VPD is projected to significantly increase over CONUS, especially in the Central U.S. (Ficklin & Novick, 2017). Figures 3b–3h present the results for the period 2060–2099 under the highest emission scenario (RCP

10.1029/2024GL113257

8.5), representing a limiting case. In the Central U.S., the interactions between UHIs and HWs are projected to be reduced because of climate warming (cf. Figures 3a to 3b, see also Figure 3c for results in the Central U.S.), which is largely attributed to the stronger inhibition of rural evapotranspiration and thus the increase of $\delta(\Delta LE)$ (cf. Figures 3d to 3e). This is further correlated with the stronger VPD during HW days than non-HW days in a warming climate (cf. Figures 3h–3g).

4. Conclusions and Discussions

In this study, whether the daily mean UHI intensity is enhanced under HWs is investigated using numerical simulations over CONUS. Results show that the daily mean UHI intensity increases under HWs over the eastern and western U.S., but decreases in the Central U.S. The increases of daily mean UHI intensity are due to the enhancement of rural evapotranspiration for the eastern U.S. and the enhancement of available energy from shortwave radiation due to less cloud and anthropogenic heat flux as air conditioning demand increases with the higher temperatures for the western U.S. under HWs. The decrease of daily mean UHI intensity in the Central U.S. is found to be related to the stronger inhibition of rural evapotranspiration by VPD stresses.

The negative interactions between UHIs and HWs were also detected by previous studies. For example, the 2012 summer heatwave induced a negative synergistic effect of 1°C–2°C in Chicago, located in the Central U.S. (K. Chen et al., 2022). Similar negative synergies have been reported in Dijon, France (Richard et al., 2021), Sydney, Australia (Kong et al., 2023), Shanghai, China (Xin et al., 2024), and various cities in India (Kumar & Mishra, 2019). Several hypotheses have been proposed to explain these negative synergistic effects, including changes in synoptic circulation, such as wind speed and direction (Kong et al., 2023; Xin et al., 2024), and reduced evapotranspiration and soil moisture in rural areas (Kumar & Mishra, 2019; Richard et al., 2021). Although the influence of VPD on the negative synergistic effect has not been emphasized in previous studies, many field studies suggest that high VPD significantly reduces evapotranspiration due to stomatal closure when VPD exceeds 2–2.5 kPa (Fletcher et al., 2007; Purdom et al., 2022). In fact, the limitation imposed by VPD on vegetation can surpass that of soil moisture in many terrestrial biomes, and this effect is expected to become more pronounced under global warming (Grossiord et al., 2020; Novick et al., 2016; Yuan et al., 2019). The critical role of VPD, along with high temperatures, in affecting rainfed crops and evapotranspiration has also been observed in the Central U.S. (Lobell et al., 2014; Sun et al., 2023). Given that urban evapotranspiration is already low due to the widespread use of impervious surfaces, the large decrease in rural evapotranspiration under high VPD conditions could further amplify the negative interactions in the Central U.S.

There are differences between findings from our study and a previous study (Zhao et al., 2018) in that we used the most recent version of the CLM model that better simulates urban processes, atmospheric forcing data with finer spatial and temporal resolution, and examined different time scales and cities. As alluded to earlier, Zhao et al. (2018) only selected 50 cities for analysis while we kept more cities/towns. Our results suggest that the sensitivity of evapotranspiration to environmental stresses is the key to understanding how the daily mean UHI intensity is altered by HWs. In particular, the role of VPD is highlighted. As a non-soil moisture factor, VPD differs from the role soil moisture plays in moderating temperatures. While studies like Zhao et al. (2018) have primarily focused on soil moisture, our work emphasizes that VPD also significantly affects evapotranspiration and temperature regulation, especially during HWs with high VPD conditions. In urban areas, where soil moisture is already limited, the impact of VPD is less pronounced because the potential for cooling via evapotranspiration is already constrained. However, in rural areas, high VPD leads to a more significant reduction in evapotranspiration, resulting in greatly increased sensible heat stress during HWs. This dynamic intensifies heat accumulation in rural areas, contributing to the negative UHI-HW interactions observed in our simulations.

Our findings also indicate that it is important for climate and earth system models to correctly represent the sensitivity of evapotranspiration to environmental stresses. The current model representation of urban and rural evapotranspiration is far from perfect, and thus our results should not be treated as the truth. For example, no urban vegetation is explicitly represented in the CLMU model and hence urban evaporation is not affected by some of the stresses that affect rural evapotranspiration (e.g., from VPD via stomatal conductance). Therefore, the interactions between UHIs and HWs may vary, as different parameterization choices or model structures could lead to varying evapotranspiration sensitivities. It is important to acknowledge that only one model is used in this study. A multi-model comparison, along with a comparison to observational data from both urban and rural sites, is needed in the future to assess the robustness of these results.

We also note the limitations of the subgrid approach, which is commonly adopted by global and regional climate models. This approach simplifies complex systems by dividing them into smaller tiles. However, such simplification can lead to the loss of detail and precision, particularly in capturing fine-scale processes. The limitations of this approach have been recognized, and high-resolution simulations could potentially address these issues, but this is beyond the scope of this study.

In this study, the role of humidity is not examined due to our focus on the traditionally defined UHIs and HWs. However, future investigations using heat stress indices that are functions of temperature and humidity (Oleson et al., 2015; Qin et al., 2023) as well as other environmental variables are welcome.

Data Availability Statement

Community Earth System Model/CLM5 release code is available online at (https://github.com/ESCOMP/CESM/tree/release-cesm2.1.3). The modified CESM/CLMU codes and post-processing scripts used in this study are publicly available at L. L. Wang and Li (2023).

Acknowledgments
Dan Li acknowledges support by the U.S. Department of Energy, Office of Science, as part of research in MultiSector Dynamics, Earth and Environmental System Modeling Program and resources of the National Energy Research Scientific Computing Center (NERSC), a U.S. Department of Energy Office of Science User Facility located at Lawrence Berkeley National Laboratory, operated under Contract No. DE-AC02-05CH11231.

References

Anderson, G. B., & Bell, M. L. (2011). Heat waves in the United States: Mortality risk during heat waves and effect modification by heat wave characteristics in 43 us communities. *Environmental Health Perspectives*, *119*(2), 210–218. https://doi.org/10.1289/ehp.1002313

Ao, X., Wang, L., Zhi, X., Gu, W., Yang, H., & Li, D. (2019). Observed synergies between urban heat islands and heat waves and their controlling factors in shanghai, China. *Journal of Applied Meteorology and Climatology*, *58*(9), 1955–1972. https://doi.org/10.1175/jamc-d-19-0073.1

Arnfield, A. J. (2003). Two decades of urban climate research: A review of turbulence, exchanges of energy and water, and the urban heat island. *International Journal of Climatology: a Journal of the Royal Meteorological Society*, *23*(1), 1–26. https://doi.org/10.1002/joc.859

Chen, K., Newman, A. J., Huang, M., Coon, C., Darrow, L. A., Strickland, M. J., & Holmes, H. A. (2022). Estimating heat-related exposures and urban heat island impacts: A case study for the 2012 chicago heatwave. *GeoHealth*, *6*(1), e2021GH000535. https://doi.org/10.1029/2021gh000535

Chen, Y., & Zhai, P. (2017). Revisiting summertime hot extremes in China during 1961–2015: Overlooked compound extremes and significant changes. *Geophysical Research Letters*, *44*(10), 5096–5103. https://doi.org/10.1002/2016gl072281

Chew, L. W., Liu, X., Li, X.-X., & Norford, L. K. (2021). Interaction between heat wave and urban heat island: A case study in a tropical coastal city, Singapore. *Atmospheric Research*, *247*, 105134. https://doi.org/10.1016/j.atmosres.2020.105134

Danabasoglu, G., Lamarque, J.-F., Bacmeister, J., Bailey, D., DuVivier, A., Edwards, J., et al. (2020). The community earth system model version 2 (cesm2). *Journal of Advances in Modeling Earth Systems*, *12*(2), e2019MS001916. https://doi.org/10.1029/2019ms001916

Ficklin, D. L., & Novick, K. A. (2017). Historic and projected changes in vapor pressure deficit suggest a continental-scale drying of the United States atmosphere. *Journal of Geophysical Research: Atmospheres*, *122*(4), 2061–2079. https://doi.org/10.1002/2016jd025855

Fletcher, A. L., Sinclair, T. R., & Allen Jr, L. H. (2007). Transpiration responses to vapor pressure deficit in well watered "slow-wilting"and commercial soybean. *Environmental and Experimental Botany*, *61*(2), 145–151. https://doi.org/10.1016/j.envexpbot.2007.05.004

Founda, D., & Santamouris, M. (2017). Synergies between urban heat island and heat waves in athens (Greece), during an extremely hot summer (2012). *Scientific Reports*, *7*(1), 10973. https://doi.org/10.1038/s41598-017-11407-6

Grimm, N. B., Faeth, S. H., Golubiewski, N. E., Redman, C. L., Wu, J., Bai, X., & Briggs, J. M. (2008). Global change and the ecology of cities. *Science*, *319*(5864), 756–760. https://doi.org/10.1126/science.1150195

Grimmond, S. (2007). Urbanization and global environmental change: Local effects of urban warming. *The Geographical Journal*, *173*(1), 83–88. https://doi.org/10.1111/j.1475-4959.2007.232_3.x

Grossiord, C., Buckley, T. N., Cernusak, L. A., Novick, K. A., Poulter, B., Siegwolf, R. T., et al. (2020). Plant responses to rising vapor pressure deficit. *New Phytologist*, *226*(6), 1550–1566. https://doi.org/10.1111/nph.16485

Hajat, S., & Kosatky, T. (2010). Heat-related mortality: A review and exploration of heterogeneity. *Journal of Epidemiology and Community Health*, *64*(9), 753–760. https://doi.org/10.1136/jech.2009.087999

Jones, A. D., Rastogi, D., Vahmani, P., Stansfield, A. M., Reed, K. A., Thurber, T., et al. (2023). Continental United States climate projections based on thermodynamic modification of historical weather. *Scientific Data*, *10*(664), 664. https://doi.org/10.1038/s41597-023-02485-5

Kalnay, E., & Cai, M. (2003). Impact of urbanization and land-use change on climate. *Nature*, *423*(6939), 528–531. https://doi.org/10.1038/nature01675

Kong, J., Zhao, Y., Carmeliet, J., & Lei, C. (2021). Urban heat island and its interaction with heatwaves: A review of studies on mesoscale. *Sustainability*, *13*(19), 10923. https://doi.org/10.3390/su131910923

Kong, J., Zhao, Y., Strebel, D., Gao, K., Carmeliet, J., & Lei, C. (2023). Understanding the impact of heatwave on urban heat in greater sydney: Temporal surface energy budget change with land types. *Science of the Total Environment*, *903*, 166374. https://doi.org/10.1016/j.scitotenv.2023.166374

Kumar, R., & Mishra, V. (2019). Decline in surface urban heat island intensity in India during heatwaves. *Environmental Research Communications*, *1*(3), 031001. https://doi.org/10.1088/2515-7620/ab121d

Lau, N.-C., & Nath, M. J. (2014). Model simulation and projection of european heat waves in present-day and future climates. *Journal of Climate*, *27*(10), 3713–3730. https://doi.org/10.1175/jcli-d-13-00284.1

Li, D., & Bou-Zeid, E. (2013). Synergistic interactions between urban heat islands and heat waves: The impact in cities is larger than the sum of its parts. *Journal of Applied Meteorology and Climatology*, *52*(9), 2051–2064. https://doi.org/10.1175/jamc-d-13-02.1

Li, D., Liao, W., Rigden, A. J., Liu, X., Wang, D., Malyshev, S., & Shevliakova, E. (2019). Urban heat island: Aerodynamics or imperviousness? *Science Advances*, *5*(4), eaau4299. https://doi.org/10.1126/sciadv.aau4299

Li, D., Sun, T., Liu, M., Yang, L., Wang, L., & Gao, Z. (2015). Contrasting responses of urban and rural surface energy budgets to heat waves explain synergies between urban heat islands and heat waves. *Environmental Research Letters*, *10*(5), 054009. https://doi.org/10.1088/1748-9326/10/5/054009

Li, D., Wang, L., Liao, W., Sun, T., Katul, G., Bou-Zeid, E., & Maronga, B. (2024). Persistent urban heat. *Science Advances*, *10*(15), eadj7398. https://doi.org/10.1126/sciadv.adj7398

Lobell, D. B., Roberts, M. J., Schlenker, W., Braun, N., Little, B. B., Rejesus, R. M., & Hammer, G. L. (2014). Greater sensitivity to drought accompanies maize yield increase in the u.s. midwest. *Science*, *344*(6183), 516–519. https://doi.org/10.1126/science.1251423

Manoli, G., Fatichi, S., Bou-Zeid, E., & Katul, G. G. (2020). Seasonal hysteresis of surface urban heat islands. *Proceedings of the National Academy of Sciences*, *117*(13), 7082–7089. https://doi.org/10.1073/pnas.1917554117

Manoli, G., Fatichi, S., Schläpfer, M., Yu, K., Crowther, T. W., Meili, N., et al. (2019). Magnitude of urban heat islands largely explained by climate and population. *Nature*, *573*(7772), 55–60. https://doi.org/10.1038/s41586-019-1512-9

Medlyn, B. E., Duursma, R. A., Eamus, D., Ellsworth, D. S., Prentice, I. C., Barton, C. V., et al. (2011). Reconciling the optimal and empirical approaches to modelling stomatal conductance. *Global Change Biology*, *17*(6), 2134–2144. https://doi.org/10.1111/j.1365-2486.2010.02375.x

Meehl, G. A., & Tebaldi, C. (2004). More intense, more frequent, and longer lasting heat waves in the 21st century. *Science*, *305*(5686), 994–997. https://doi.org/10.1126/science.1098704

Miralles, D. G., Gentine, P., Seneviratne, S. I., & Teuling, A. J. (2019). Land–atmospheric feedbacks during droughts and heatwaves: State of the science and current challenges. *Annals of the New York Academy of Sciences*, *1436*(1), 19–35. https://doi.org/10.1111/nyas.13912

Novick, K. A., Ficklin, D. L., Stoy, P. C., Williams, C. A., Bohrer, G., Oishi, A. C., et al. (2016). The increasing importance of atmospheric demand for ecosystem water and carbon fluxes. *Nature Climate Change*, *6*(11), 1023–1027. https://doi.org/10.1038/nclimate3114

Oke, T. R. (1982). The energetic basis of the urban heat island. *Quarterly Journal of the Royal Meteorological Society*, *108*(455), 1–24. https://doi.org/10.1002/qj.49710845502

Oke, T. R., Mills, G., Christen, A., & Voogt, J. A. (2017). *Urban climates*. Cambridge University Press.

Oleson, K. W., Bonan, G. B., & Feddema, J. (2010). Effects of white roofs on urban temperature in a global climate model. *Geophysical Research Letters*, *37*(3). https://doi.org/10.1029/2009gl042194

Oleson, K. W., Bonan, G. B., Feddema, J., & Jackson, T. (2011). An examination of urban heat island characteristics in a global climate model. *International Journal of Climatology*, *31*(12), 1848–1865. https://doi.org/10.1002/joc.2201

Oleson, K. W., Bonan, G. B., Feddema, J., & Vertenstein, M. (2008). An urban parameterization for a global climate model. part ii: Sensitivity to input parameters and the simulated urban heat island in offline simulations. *Journal of Applied Meteorology and Climatology*, *47*(4), 1061–1076. https://doi.org/10.1175/2007jamc1598.1

Oleson, K. W., Bonan, G. B., Feddema, J., Vertenstein, M., & Grimmond, C. (2008). An urban parameterization for a global climate model. part i: Formulation and evaluation for two cities. *Journal of Applied Meteorology and Climatology*, *47*(4), 1038–1060. https://doi.org/10.1175/2007jamc1597.1

Oleson, K. W., Bonan, G. B., Feddema, J., Vertenstein, M., & Kluzek, E. (2010). Technical description of an urban parameterization for the community land model (clmu). *NCAR, Boulder*, *10*, D6K35RM9.

Oleson, K. W., & Feddema, J. (2020). Parameterization and surface data improvements and new capabilities for the community land model urban (clmu). *Journal of Advances in Modeling Earth Systems*, *12*(2), e2018MS001586. https://doi.org/10.1029/2018ms001586

Oleson, K. W., Monaghan, A., Wilhelmi, O., Barlage, M., Brunsell, N., Feddema, J., et al. (2015). Interactions between urbanization, heat stress, and climate change. *Climatic Change*, *129*(3–4), 525–541. https://doi.org/10.1007/s10584-013-0936-8

Perkins, S. E. (2015). A review on the scientific understanding of heatwaves—Their measurement, driving mechanisms, and changes at the global scale. *Atmospheric Research*, *164*, 242–267. https://doi.org/10.1016/j.atmosres.2015.05.014

Purdom, S., Shekoofa, A., McClure, A., Pantalone, V., Arelli, P., & Duncan, L. (2022). Variation in mid-south soybean genotypes for recovery of transpiration rate and leaf maintenance following severe water-deficit stress. *Field Crops Research*, *286*, 108625. https://doi.org/10.1016/j.fcr.2022.108625

Qin, Y., Liao, W., & Li, D. (2023). Attributing the urban–rural contrast of heat stress simulated by a global model. *Journal of Climate*, *36*(6), 1805–1822. https://doi.org/10.1175/jcli-d-22-0436.1

Ramamurthy, P., & Bou-Zeid, E. (2017). Heatwaves and urban heat islands: A comparative analysis of multiple cities. *Journal of Geophysical Research: Atmospheres*, *122*(1), 168–178. https://doi.org/10.1002/2016jd025357

Richard, Y., Pohl, B., Rega, M., Pergaud, J., Thévenin, T., Emery, J., et al. (2021). Is urban heat island intensity higher during hot spells and heat waves (dijon, France, 2014–2019)? *Urban Climate*, *35*, 100747. https://doi.org/10.1016/j.uclim.2020.100747

Rogers, A., Medlyn, B. E., Dukes, J. S., Bonan, G., Von Caemmerer, S., Dietze, M. C., et al. (2017). A roadmap for improving the representation of photosynthesis in earth system models. *New Phytologist*, *213*(1), 22–42. https://doi.org/10.1111/nph.14283

Schatz, J., & Kucharik, C. J. (2015). Urban climate effects on extreme temperatures in madison, Wisconsin, USA. *Environmental Research Letters*, *10*(9), 094024. https://doi.org/10.1088/1748-9326/10/9/094024

Scott, A. A., Waugh, D. W., & Zaitchik, B. F. (2018). Reduced urban heat island intensity under warmer conditions. *Environmental Research Letters*, *13*(6), 064003. https://doi.org/10.1088/1748-9326/aabd6c

Sun, W., Fleisher, D., Timlin, D., Ray, C., Wang, Z., Beegum, S., & Reddy, V. (2023). Projected long-term climate trends reveal the critical role of vapor pressure deficit for soybean yields in the us midwest. *Science of the Total Environment*, *878*, 162960. https://doi.org/10.1016/j.scitotenv.2023.162960

Vahmani, P., Jones, A. D., & Li, D. (2022). Will anthropogenic warming increase evapotranspiration? Examining irrigation water demand implications of climate change in California. *Earth's Future*, *10*(1), e2021EF002221. https://doi.org/10.1029/2021ef002221

Wang, L., Huang, M., & Li, D. (2020). Where are white roofs more effective in cooling the surface? *Geophysical Research Letters*, *47*(15), e2020GL087853. https://doi.org/10.1029/2020gl087853

Wang, L., Huang, M., & Li, D. (2021). Strong influence of convective heat transfer efficiency on the cooling benefits of green roof irrigation. *Environmental Research Letters*, *16*(8), 084062. https://doi.org/10.1088/1748-9326/ac18ea

Wang, L., & Li, D. (2023). Clmu interactions between uhis and hws experiments [Dataset]. *MSD-LIVE Data Repository*. Retrieved from https://doi.org/10.57931/1970168

Wang, P., Li, D., Liao, W., Rigden, A., & Wang, W. (2019). Contrasting evaporative responses of ecosystems to heatwaves traced to the opposing roles of vapor pressure deficit and surface resistance. *Water Resources Research*, *55*(6), 4550–4563. https://doi.org/10.1029/2019wr024771

Xin, J., Zhang, Y., Bai, W., & Song, Z. (2024). Response of urban heat island effects within the planetary boundary layer to heat waves and impact of horizontal advection over shanghai. *Atmospheric Research*, *311*, 107721. https://doi.org/10.1016/j.atmosres.2024.107721

Yuan, W., Zheng, Y., Piao, S., Ciais, P., Lombardozzi, D., Wang, Y., et al. (2019). Increased atmospheric vapor pressure deficit reduces global vegetation growth. *Science Advances*, *5*(8), eaax1396. https://doi.org/10.1126/sciadv.aax1396

Zhao, L., Lee, X., Smith, R. B., & Oleson, K. (2014). Strong contributions of local background climate to urban heat islands. *Nature*, *511*(7508), 216–219. https://doi.org/10.1038/nature13462

10.1029/2024GL113257

Zhao, L., Oppenheimer, M., Zhu, Q., Baldwin, J. W., Ebi, K. L., Bou-Zeid, E., et al. (2018). Interactions between urban heat islands and heat waves. *Environmental Research Letters*, *13*(3), 034003. https://doi.org/10.1088/1748-9326/aa9f73

Zhou, D., Zhang, L., Li, D., Huang, D., & Zhu, C. (2016). Climate–vegetation control on the diurnal and seasonal variations of surface urban heat islands in China. *Environmental Research Letters*, *11*(7), 074009. https://doi.org/10.1088/1748-9326/11/7/074009

Zhou, L., Dickinson, R. E., Tian, Y., Fang, J., Li, Q., Kaufmann, R. K., et al. (2004). Evidence for a significant urbanization effect on climate in China. *Proceedings of the National Academy of Sciences*, *101*(26), 9540–9544. https://doi.org/10.1073/pnas.0400357101